FABRICATION OF A-SI SOLAR CELLS WITH RF- AND MW-PECVD

B.B. Van Aken, M. Dörenkämper, C. Devilee, M.C.R. Heijna, J. Löffler and W.J. Soppe
ECN Solar Energy, P.O. Box 1, 1755 ZG Petten, the Netherlands,
Phone: +31 224 56 4905, Fax: +31 224 56 8214, E-mail: vanaken@ecn.nl

Roll-to-roll production technology specifically designed to produce thin film Si solar cells should lead to a significant reduction of the module production costs. At ECN we developed a roll-to-roll Si coating system which contains novel, linear RF sources for the deposition of n- and p-type silicon layers and linear MW sources for the deposition of intrinsic silicon layers. The quality and uniformity of doped and intrinsic silicon layers that are grown by these linear plasma sources are discussed. The layer quality confirms that the RF and MW sources in the roll-to-roll coater are suitable for the growth of micromorph Si solar cells. Preliminary results on amorphous silicon solar cells are presented with an initial efficiency of 4.4%.
Keywords: RF- & MW-PECVD, a-Si:H, thin film solar cells, roll-to-roll technology

1 INTRODUCTION

Roll-to-roll production of thin film Si solar cells has several advantages over batch-type reactor systems, for instance high-throughput fabrication and the opportunity to make lightweight and flexible products. Flexible and lightweight PV modules gear up to building integrated PV: the most important market for PV in densely populated, developed countries [1, 2]. ECN is developing a pilot line for roll-to-roll production of high efficiency n-i-p solar cells based on amorphous (a-Si:H) and microcrystalline (μc-Si:H) silicon thin films on steel foil coated with an insulating barrier layer and sputtered back contact and reflection layer. As part of the pilot line, we have developed, in collaboration with Roth&Rau AG, a roll-to-roll PECVD system, the FLEXICOAT300, for the Si layer deposition [3].

This contribution focuses on two aspects of our research programme: p-type Si layers and the fabrication of p-i-n and n-i-p a-Si solar cells. In the first part, the relation between the deposition conditions of the RF-PECVD process and the optical, structural and electronic properties of p-type a-Si:H, a-SiC:H and μc-Si:H layers are discussed, in order to identify optimal conditions for growth of device quality p-type layers. The second part covers the first results for p-i-n a-Si solar cells deposited on Asahi-U superstrates, with both a-Si:H and a-SiC p-type window layers

2 EXPERIMENTAL

2.1 Deposition process

The FLEXICOAT300 has three deposition chambers and can handle webs with a width up to 30 cm (see sketched cross-section in Figure 1). The intrinsic layers are deposited by microwave (MW) PECVD as this combines good quality and uniformity with high deposition rates [4]. However, this linear MW source is not suitable for deposition of doped layers, as the quartz tube, shielding the antenna, does not transmit EM radiation when covered by a highly conductive (doped silicon) layer. A novel, linear RF source has been developed to circumvent this problem [5]. Just as the linear microwave sources, these symmetric RF sources do not require the grounding of the substrate, and the indirect plasma causes only a very mild ion bombardment on the surface of the substrate or growing layer. The lower deposition rates for RF-PECVD with respect to MW-PECVD are not a bottle-neck in high-throughput processing since the thicknesses of doped layers in thin film Si solar cells are small (≤ 20 nm) with respect to the required thickness of the intrinsic layer (≥ 1 μm for μc-Si).

The foil moves in continuous mode through the chambers and in order to prevent cross contamination of process gases, gas gates are applied between the deposition chambers.

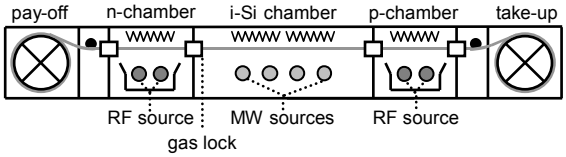

Figure 1: Cross-section through the FLEXICOAT300 roll-to-roll coater. Both RF sources, in the n- and p-chamber, contain two parallel linear electrodes, whereas the four MW sources have one antenna each in a quartz tube.

2.2 Characterisation

For layer optimisation, three 3 × 3 cm^2 samples have been deposited simultaneously, one on a double-sided polished CZ Si wafer and two on Corning 2000 glass. The quality of the layers was examined by a range of techniques. Si p-i-n layer stacks were deposited on Asahi-U glass, followed by e-beam PVD of Ag/Al back contacts through a mask, which defined the dimensions of the individual solar cells, 4 × 4 mm^2.

Fourier transform infrared spectroscopy (FTIR) spectra were recorded with a Perkin Elmer BX II spectrometer between 400 cm^{-1} and 4000 cm^{-1}. By fitting of the spectra the layer thickness d, refractive index $n@0.5\ eV$ and extinction coefficient k are obtained.

The temperature dependence (393-273 K) of the dark conductivity σ_d is measured during a cooling run after annealing at 393 K for 2 hours in a vacuum chamber to prevent oxidation and minimise the effect of water vapour. The activation energy E_{act} is calculated from a linear fit to the Arrhenius plot. Reflectance and transmittance (R-T) are measured using an integrating sphere to obtain the absorption spectra in the range 400-1400 nm and determine the optical gap E_g from the Tauc plot. Raman spectra have been measured by a Renishaw InVia Raman microscope using λ = 514 nm light from a 20 mW laser. The crystalline volume fraction ϕ_c is calculated from the ratio of the amorphous and crystalline contributions according to

$$\phi_c = \frac{I_{520} + I_{505}}{I_{520} + I_{505} + I_{480}} \qquad (1)$$

where I_n is the intensity of the peak at n cm^{-1}.

I-V curves are measured in dark with a Keithley2400 sourcemeter and under AM1.5 conditions using a Xenon arc solar simulator (Oriel-81172).

Uniformity of the layers over the full width of the web has been analysed by reflection measurements to evaluate the thickness. Further, we have examined the usage of surface photovoltage (SPV) measurements to analyse the uniformity of the electronic properties of the layers. The measurements were made with an ambient Kelvin probe (KP Technology) with a probe area of about 0.8 cm^2, under illumination with a halogen lamp.

3 RESULTS AND DISCUSSION

3.1 Uniformity of the depositions

The linear RF source can be operated in the power range between 100 and 600 Watt and provides very homogeneous depositions over the entire width of the web. A typical example is given in Figure 2. The linear MW sources can be operated between 100 and 2000 W, but a certain minimum power is required to obtain homogeneous depositions. This minimum power depends on the pressure and on the process gases being used (i.e. it depends on the power absorption by the plasma), but the typical minimum power is in the range between 750 and 1000 W per generator (Note that the MW source is fed with two MW generators, one frontside and one on the rear side of the source). If this minimum power requirement is met, very homogeneous layers with thickness variation of less than 5% over the width of the web can be obtained.

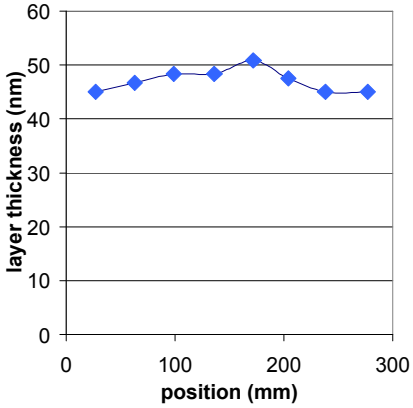

Figure 2: Thickness variation of an a-Si layer grown with the linear RF source. The variation is less than 4%.

We have performed ex-situ SPV measurements of intrinsic silicon layers over the entire width of the web, to investigate the suitability of this method for in-situ quality control. In Figure 3 we present SPV data for an inhomogeneous layer and we observe that in this case the SPV signal follows the behaviour of the thickness of the layer. This probably implies that for this deposition, the electronic quality of the layer is uniform over the entire width. This however still has to be verified by independent photoconductivity measurements.

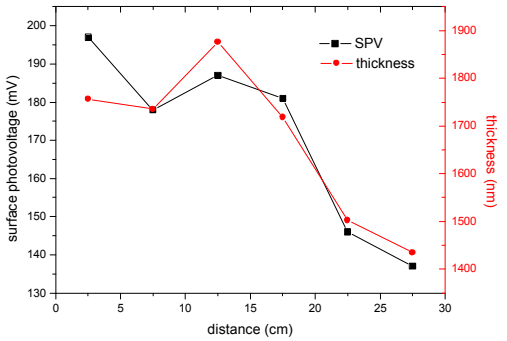

Figure 3: SPV results and thickness data for an inhomogeneous layer.

3.2 p-type Si layers

We have succeeded in growing p-type a-Si:H layers by doping with diborane, B_2H_6, applying the linear RF-PECVD source. The growth rate r_d is typically ~0.4 Å/s. Table I gives an overview of the relevant material properties of these a-Si:H layers in the last column.

Compared to intrinsic a-Si:H, boron-doped p-type a-Si:H has a lower band gap and a higher absorption at $\lambda = 600$ nm. As the p-type layer is applied as window layer in thin film a-Si solar cells, a high absorption in the p-layer decreases the number of charge carriers created in the intrinsic layer. Furthermore, the low band gap causes some back diffusion of electrons. Both effects lower the efficiency of solar cells with p-type a-Si:H window layers.

Table I: Overview of p-type Si:H layers made by the novel linear RF source. *) The Tauc gap E_g is not well-defined for mixed µc-Si/a-Si material. The absorption α is taken at 600 nm.

Material parameter	µc-Si:H p-type	a-SiC p-type	a-Si:H p-type
σ_d [S/cm]	6×10^{-1}	5×10^{-7}	3×10^{-4}
E_{act} [eV]	0.06	0.40	0.19
E_g [eV]	*)	1.91	1.74
α [10^4 cm^{-1}]	1.2	2.1	2.4
ϕ_c [%]	55	0	0
r_d [Å/s]	0.34	0.71	0.51
d [nm]	195	190	230

To overcome these problems, p-doped a-SiC is commonly used as window layer. We fabricated SiC layers by adding methane to the deposition chamber. However, the addition of carbon in the amorphous silicon network is detrimental for the conducting properties. Figure 4 shows the effect of CH_4 and B_2H_6 on the optical and electronic properties of p-type layers. For a number of samples, covering a large range of CH_4 and B_2H_6 flows, σ_d and E_{act} are plotted as a function of E_g. Ideal samples have high conductivity and low activation energy. Clearly, an improvement in the optical properties is accompanied with a decline in the conducting properties. The optimal combination has to be found by comparing several of these p-type layers in a-Si solar cells.

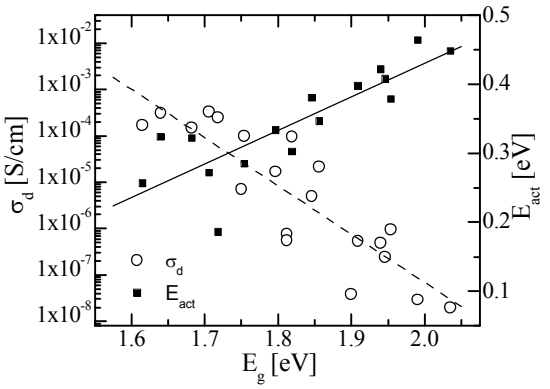

Figure 4: σ_d (left axis, open circles) and E_{act} (right axis, solid squares) as a function of E_g. The lines are linear fits: increasing CH_4 flow or decreasing B_2H_6 flow results in a higher E_g, but a lower σ_d and higher E_{act}.

In Figure 5, the absorption of the p-layers is plotted against the photon energy in a so-called Tauc plot. We see that the absorption coefficient α is somewhat lower for a-SiC than for p-type a-Si:H. Application of these a-SiC layers in solar cells should increase the light transmitted through the p-type layer and into the intrinsic layer. This will increase the carrier generation, as shown later in Figure 7.

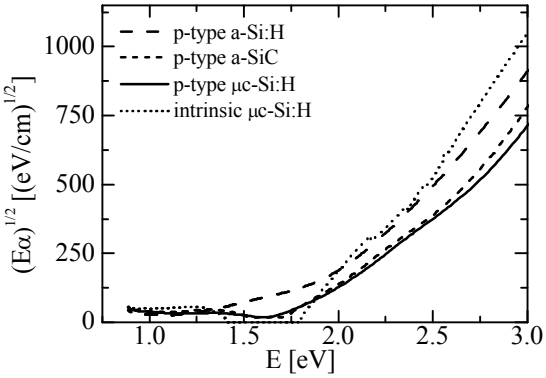

Figure 5: Tauc plot, $(E\alpha)^{1/2}$ as a function of E [6], of the samples shown in Table 1. The a-Si:H sample has an order of magnitude higher absorption compared with the other three samples.

Next to the development of amorphous p-layers, an objective of this study is the development of microcrystalline p-type layers for application in single junction a-Si and μc-Si solar cells, and a-Si/μc-Si tandem solar cells. We deposited 100 nm intrinsic μc-Si:H layers by RF-PECVD on glass substrates to act as seed layers. After conditioning the chamber, p-type μc-Si:H layers were deposited in the same chamber. Figure 6 shows Raman spectra for the seed layer and the combined p-type/seed layer samples. For reference, also the spectra for p-doped a-Si:H and a-SiC:H layers are given. The p-type μc-Si:H layer has only a slightly lower crystalline fraction than the intrinsic seed layer.

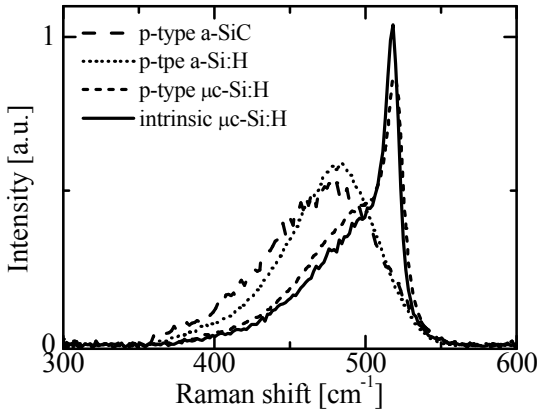

Figure 6: Raman spectra of the samples shown in Table **I**. The sharp peak at ~518 cm^{-1} is due to the TO mode in crystalline Si, the much broader peak at 480 cm^{-1} is due to the TO mode in a-Si:H. Layer thicknesses are about ~200 nm and given in Table I.

Besides a minimal crystalline fraction, the p-type μc-Si:H layer should also have a high conductivity and low activation energy. In Table I, the electronic properties of the p-type μc-Si:H layer are shown. The addition of B_2H_6 causes an increase of σ_d by 4 orders of magnitude and a significant decrease of E_{act} relative to the intrinsic μc-Si:H layer. The Raman and conductivity measurements indicate that the p-doping is successful and does not inhibit crystalline growth.

To summarise the p-type layer deposition with linear RF-sources for PECVD: we have succeeded in growing device quality a-SiC layers, with E_g > 1.90 eV and E_{act} ~ 0.42 eV. Furthermore, we have shown that p-type μc-Si:H layers with good electronic properties and ϕ_c ~ 55% can be grown on intrinsic μc-Si:H seed layers.

3.3 a-Si solar cells

The optimised deposition processes were applied to produce thin film Si solar cells with intrinsic layers, grown with the linear MW sources, and doped layers, deposited with the linear, asymmetric RF sources. Figure 7 shows I-V characteristics obtained on some of these cells. The cell that incorporates a p-type a-Si:H window layer (dotted line), not only has a low I_{sc}, but also a very low V_{oc}.

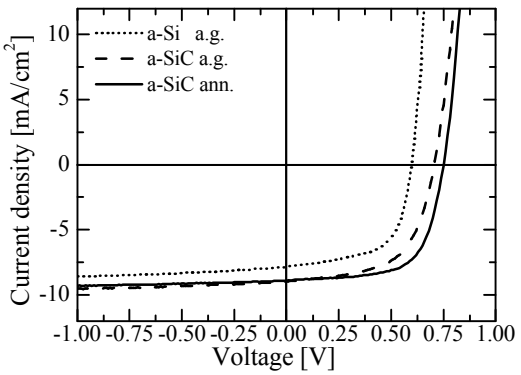

Figure 7: I-V curves for a-Si solar cells with an a-Si:H window layer (as grown: dotted), an a-SiC window layer (as grown: dashed) and the a-SiC solar cell after annealing (solid).

Table II gives an overview of the cell parameters for three solar cells, taken from the IV characteristics in Figure 7. We learn from the IV-curves and the table that replacing the p-type a-Si:H window layer by a p-type a-SiC layer, increases the voltage over the cell, because of the higher band gap of a-SiC that reduces the back diffusion of electrons and also leads to a higher built-in voltage between the p and i-layer. It also increases the short-circuit current by more than 10%. This is a strong indication that the carrier generation has improved. Furthermore, the shunt resistance increases, compared with the a-Si solar cell.

Table II: I-V characteristics for a-Si solar cells with p-type a-Si:H and a-SiC window layers. FF stands for fill factor. As-grown and annealed samples are indicated by (a.g.) and (ann.), respectively.

	V_{oc} [mV]	I_{sc} [mA/cm^2]	FF [%]	η [%]
a-Si (a.g.)	600	7.8	61	2.9
a-SiC (a.g.)	710	8.9	60	3.7
a-SiC (ann.)	750	8.9	66	4.4

However, we also observe that the series resistance increases, which has a negative effect on the fill factor and the V_{oc}. It turns out that after a thermal annealing step, which is common practice in industrial thin film a-Si solar cell production, the series resistance improves, leading to an improved V_{oc} and a higher fill factor.

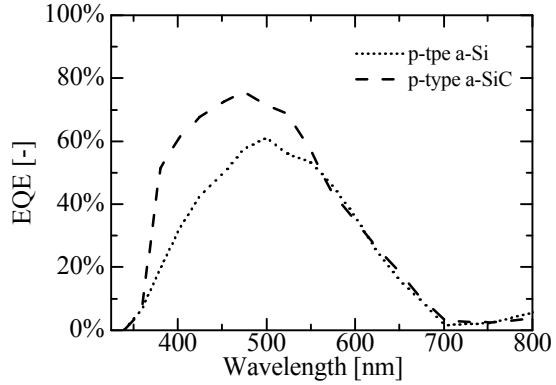

Figure 8: EQE curves for the two solar cells shown in Figure 7, after annealing. Solid and dashed lines represent the solar cells with the a-Si:H and a-SiC:H p-type window layers, respectively.

The external quantum efficiencies EQE of the a:Si solar cells have been determined from spectral response measurements, as shown in Figure 8. The EQE also reflects the improved transmittance and current collection because of the better transparent a-SiC window layer in the a-Si solar cells.

4 CONCLUSION

Using the FLEXICOAT300, a roll-to-roll PECVD system for Si layer deposition, we have found process conditions for the novel, symmetric RF sources to deposit device quality p-type Si, yielding both a-SiC and μc-Si:H layers. Amorphous silicon solar cells have been deposited for the first time applying MW-PECVD for the deposition of intrinsic layers. As-grown initial efficiencies of 3.7% have been achieved with p-type a-SiC window layers. The cell performance is improved by thermal annealing to 4.4%.

Furthermore, the first trial depositions of thin film Si layers on bare steel substrates and on steel substrates, coated by an insulating layer and a sputtered Ag/ZnO back contact, are ongoing.

5 ACKNOWLEDGEMENTS

This work has been financially supported by the Dutch Ministry of Economic Affairs (project no's. EOSLT07036 and TSIN3043) and by the European Commission under contract no. FP6-2006-Energy 3-019948.

6 REFERENCES

[1] M. Izu and T. Ellison, Sol. En. Mat. Sol. Cells **78**, 613 (2003).
[2] A. Takano and T. Kamoshita, Jap. J. Appl. Phys. **43**, 7976 (2004).
[3] W.J. Soppe et al., Proc. 17th PV SEC, Fukuoka, Japan (2007).
[4] H. Schlemm, A. Mai, S. Roth, D. Roth, K.-M. Baumgärtner and H. Muegge, Surf. Coat. Tech. **174-175,** 208 (2003).
[5] H. Schlemm, M. Fritzsche and D. Roth, Surf. Coat. Tech. **200**, 958 (2005).
[6] J. Tauc, R. Grigorovici and A. Vancu, Phys. Stat. Sol. **15**, 627 (1966).